

Chapter 7

To What Extent will Projected Changes in Global Emissions Affect Mercury Levels in the Arctic Atmosphere and Ocean?

COORDINATING AUTHORS: JOZEF M. PACYNA, KYRRE SUNDSETH

CO-AUTHORS: JESPER CHRISTENSEN, ASHU DASTOOR, ROBIE MACDONALD, JOHN MUNTHE, ANDREW RYZHKOV, OLEG TRAVNIKOV, SIMON WILSON

7.1. Introduction

For policy-makers to decide whether and how best to implement strategies to reduce environmental pollutants such as mercury (Hg), information is required on a number of factors, including possible future developments. From an Arctic perspective, projections of future global emissions of Hg and how these may affect levels of Hg in the region's atmosphere and ocean are therefore important questions to address in this assessment. In addition, in order to evaluate the effectiveness of possible reductions in anthropogenic Hg emissions, it is necessary to consider how long it might take for the Arctic atmosphere and ocean to respond to source reduction measures. As long as global economic activities continue to increase, and current patterns, practices and uses are maintained, Hg pollution will undoubtedly increase in the future. There are however, various ways to reduce Hg emissions and their negative impacts on the environment and human health. Often the question is how to allocate limited resources to reducing Hg emissions in the most cost-effective manner possible.

7.2. How are anthropogenic mercury emissions likely to change in the future?

The AMAP/UNEP project *Global Atmospheric Mercury Assessment: Sources, Emissions and Transport* (UNEP, 2008; Pacyna et al., 2010a) included a first attempt to construct global emissions inventories for the year 2020 in order to investigate the implications of action to reduce Hg emissions. This section outlines the main results.

Future Hg emissions are dependent upon a number of variables, including the development of national and regional economies, the development and implementation of technologies for reducing Hg emissions, possible regulatory changes, and factors connected to global climate change.

As a first attempt to gain insight into the possible implications for global anthropogenic emissions of Hg to the atmosphere, of taking (additional) actions *vs.* not taking (additional) actions to control emissions, three emissions scenarios were considered for the target year of 2020: the 'Status Quo' (SQ) scenario, the 'Extended Emissions Control' (EXEC) scenario, and the 'Maximum Feasible Technological Reduction' (MFTR) scenario.

- The SQ scenario assumes that current patterns, practices and uses that result in Hg emissions to air will continue. Economic activity is assumed to increase in various regions; however, emission control practices remain unchanged from

those currently employed, leading to increased emissions from several sectors.

- The EXEC scenario assumes economic progress at a rate reflecting the future development of industrial technologies and emissions control technologies; that is, Hg-reducing technologies currently generally employed throughout Europe and North America would be implemented elsewhere. It further assumes that emissions control measures currently committed to in Europe to reduce Hg emissions to air or water would be implemented throughout the world. These include certain measures adopted under the Heavy Metals Protocol to the UNECE Convention on Long-range Transboundary Air Pollution (LRTAP), EU Directives, and agreements to meet targets set by the Kyoto Protocol to the United Nations Framework Convention on Climate Change on reduction of greenhouse gases causing climate change (which will also result in reductions in Hg emissions).
- The MFTR scenario assumes implementation of all available solutions/measures, leading to the maximum degree of reduction in Hg emissions and Hg discharges to any environment; cost is taken into account but only as a secondary consideration.

Table 7.1 summarizes the assumptions made for Hg emissions in 2020.

Scenario estimates of by-product (and chlor-alkali) sector emissions of Hg in 2020 for the three scenarios (SQ, EXEC, MFTR) are presented for different regions in Figure 7.1. The scenario emissions inventories were based on the 2005 (v5) global inventory of anthropogenic Hg emissions to air produced as part of a joint UNEP project in 2008 (UNEP, 2008; see also Section 2.2). The 2005 (v5) emissions estimates are included in Figure 7.1 for comparison.

If no major changes in the efficiency of emission control are introduced and economic activity continues to increase (the SQ scenario), significant increases in global anthropogenic Hg emissions (equivalent to about one quarter of the 2005 Hg emissions from these sectors) are projected for 2020. The greatest increase is projected for stationary combustion, mainly from combustion of coal. A comparison of the 2020 emissions projected by the EXEC scenario (850 t) and the SQ scenario (1850 t) suggests that a further 1000 t of Hg could be emitted globally in 2020, if Hg continues to be emitted under the control measures and practices that are in operation today against a backdrop of increasing population and economic growth in some regions. In other words, implementation of available measures and practices (the basic assumption of the EXEC scenario), implies a reduction in Hg emissions of up to 1000 t/y in the period to 2020. The difference between the SQ

Table 7.1. Scenario assumptions for mercury emissions in 2020 (UNEP, 2008).

Sector	SQ 2020	EXEC 2020	MFTR 2020
Large combustion plants	Increase in coal consumption in Africa (20%), South America (50%) and Asia (50%). Application of current technology.	SQ 2020 + De-dusting: fabric filters (FFs) and electrostatic precipitators (ESPs) operated in combination with flue gas desulfurization (FGD). Activated carbon filters. Sulfur-impregnated absorbents. Selenium-impregnated filters.	SQ 2020 + Integrated gasification combined cycle (IGCC). Supercritical polyvalent technologies. 50% participation in electricity generation by thermal method.
Iron and steel production	Application of current technology.	In sintering: fine wet scrubbing systems or FFs with addition of lignite coke powder. In blast furnaces (BF): scrubbers or wet ESPs for BF gas treatment. In basic oxygen furnace: dry ESP or scrubbing for primary de-dusting and FFs or ESPs for secondary de-dusting. In electric arc furnaces: FFs and catalytic oxidation.	EXEC 2020 techniques in existing installations plus: Sorting of scrap. New iron-making techniques. Direct reduction and smelting reduction.
Cement industry	Increase in global cement production (50%).	SQ 2020 plus: De-dusting: FFs and ESPs.	SQ 2020 and EXEC 2020 plus: All plants with techniques for heavy metals reduction.
Chlor-alkali industry	Application of current technology.	Phase-out of mercury-cell plants by 2010	Phase-out of mercury-cell plants by 2010

Mercury emissions, tonnes

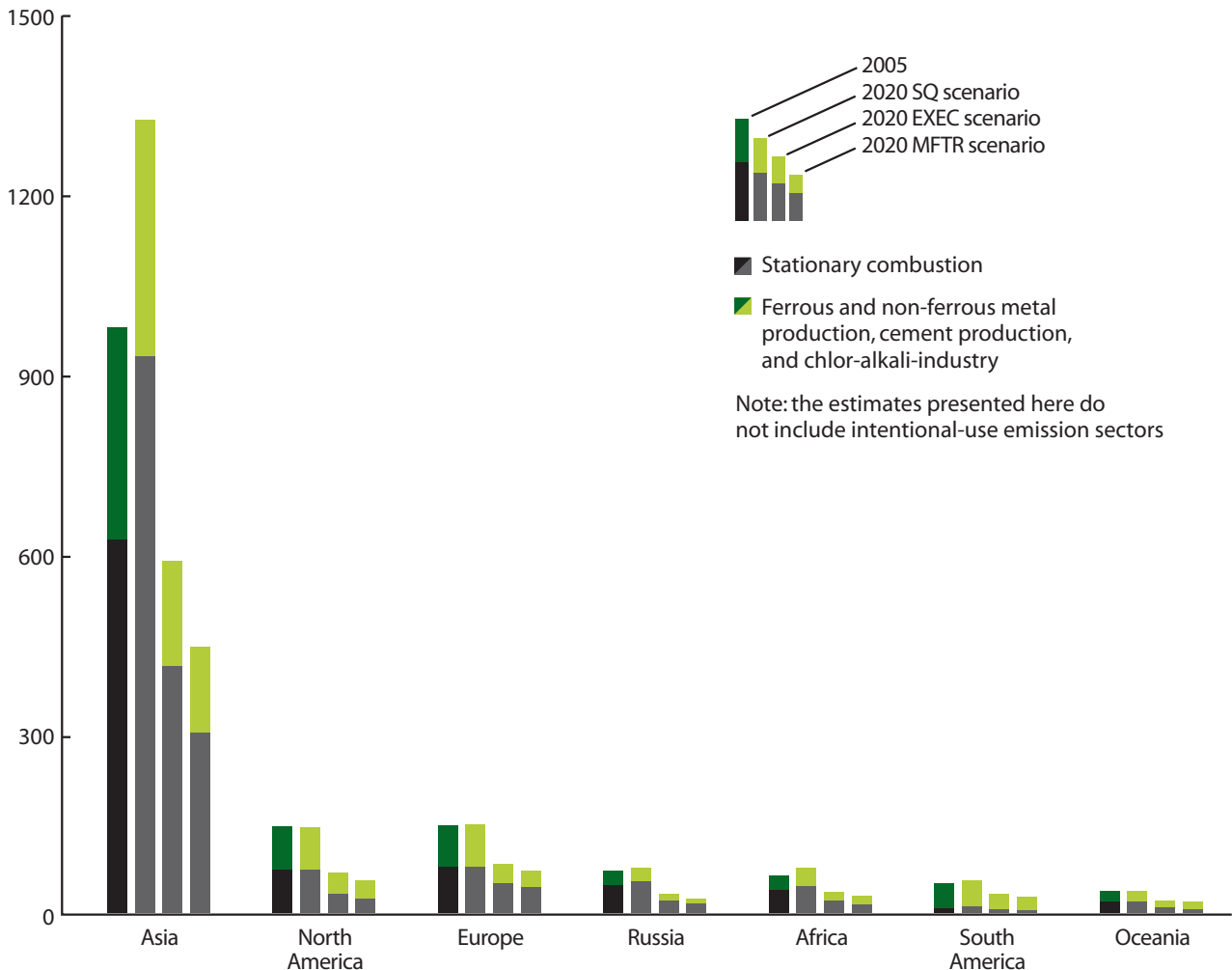


Figure 7.1. Comparison of anthropogenic emissions of mercury from the 'by-product' plus chlor-alkali sectors in 2005 and as projected under the 2020 SQ, EXEC and MFTR scenarios (UNEP, 2008).

scenario and the MFTR scenario is even greater. In this case, Hg emissions from various industrial sectors (e.g., cement production and metal manufacturing) could be 2- to 3-fold higher by 2020 if nothing is done to improve emission control.

Under the EXEC scenario, clear decreases in Hg emissions between 2005 and 2020 are projected for all continents (Figure 7.1), with the greatest Hg emissions in 2020 still projected to occur in Asia. Emissions in China (almost 635 t in 2005) are projected to decrease by 2020 to between 380 t (EXEC scenario; 40% reduction) and 290 t (MFTR scenario; 55% reduction). The projections assume that by 2020 all Chinese power plants will be equipped with improved emission control installations, and that coal consumption and industrial production in China will increase by factors of 2 and 1.5, respectively, between 2005 and 2020. The projections are also based on rigorous implementation of emissions reduction measures, particularly concerning major improvement in the efficiency of emission controls installed. This means that, if the improvement is (for example) 50% lower than assumed under the EXEC and MFTR scenarios, Chinese emissions will increase rather than decrease by 2020 (i.e., reductions due to emission control would not compensate for the projected increase in emissions due to economic development).

Similar assumptions were made in scaling emission factors according to projected improvement in the efficiency of emission controls installed at Indian power stations and industrial plants by 2020.

Projected decreases in Hg emissions in Europe, North America, Australia, Japan and Russia are between 40% and 60%.

An increase of up to 96% in global Hg emissions by 2050 relative to 2006 has been projected by Streets et al. (2009) using a range of assumptions on socio-economic and technological development. Streets and co-workers identified the expansion of coal-fired electricity generation in the developing world, particularly Asia, as the main driving force for this increase. Their projections imply a shift in the speciation of the emissions, with the share of elemental Hg declining relative to divalent Hg species, possibly due to a change from long-range transport to deposition closer to sources.

Since projections of future global emissions of Hg are necessarily based on a range of assumptions concerning national and regional economic development, the development and implementation of emission control technology, and possible regulatory change, they can only be hypothetical in nature. Furthermore, assumptions about the ambition level for emission reductions (especially in developing regions/countries) as well as willingness to invest in emission reduction measures, can result in over-optimistic reduction scenarios. Nevertheless, the scenarios illustrate well the differences between 'action' vs 'no action' in terms of reducing Hg emissions.

Scenarios for future intentional use of Hg are highly uncertain due to the lack of consistent international agreements or policies to reduce Hg demand. Although large efforts are being made in many countries to reduce Hg use in products and industrial applications, actual compliance is difficult to estimate.

7.3. How will future changes in global emissions and climate affect mercury levels in the Arctic atmosphere?

7.3.1. Arctic atmospheric mercury concentrations under different emissions scenarios for 2020

Three global Hg models (GRAHM, Environment Canada; GLEMOS, Meteorological Synthesizing Centre-East; DEHM, Danish National Environmental Research Institute; DMU/NERI) were employed to analyze the impact of the SQ, EXEC and MFTR emissions scenarios on Hg levels in the Arctic atmosphere relative to the baseline scenario for 2005. The models represent the atmospheric components of the global Hg cycle, including emissions from anthropogenic and natural sources and re-emissions of previously deposited Hg (originating both from anthropogenic and natural sources), atmospheric transport, chemical transformations, and deposition to terrestrial and ocean surfaces. Descriptions of the models' parameterizations are given in Section 2.6.1. With respect to uncertainties in the atmospheric models, the relative importance of the various potential atmospheric oxidants of gaseous elemental Hg (GEM) (O_3 , OH, H_2O_2 and reactive halogen species: Br, Cl, I, Br_2 , Cl_2 , BrO, ClO, IO, etc.) is currently insufficiently understood and represents one of the largest potential sources of error in model predictions. The size and mechanisms of natural emissions and re-emissions of Hg are also unclear and present an equally significant source of uncertainty in the models. Chapter 2 provides a more detailed discussion of model uncertainties (Section 2.6.1.2) and summarizes the main differences between the GRAHM, DEHM and GLEMOS models (Table 2.5).

Estimates of Hg emissions in 2005 (the baseline year) and emissions scenarios for 2020 in the SQ, EXEC and MFTR schemes were used in similar runs in the three models (GRAHM, GLEMOS, DEHM) to estimate annual average concentrations of GEM for 2005 and 2020. The models used the anthropogenic emissions reported in Section 7.2, but each model used its own estimates of natural and revolatilized emissions. The model estimates were performed keeping the global meteorological conditions the same for all simulations. The meteorology for 2005 was used as a reference and so no account was made for the impact of climate change during the period 2005 to 2020. The impact of change in anthropogenic emissions on re-emissions from terrestrial and oceanic surfaces was included in the GLEMOS model and shown to be negligible.

The overall global Hg emissions are projected to increase by 19% between 2005 and 2020 under the SQ scenario. In contrast, global emissions are projected to decrease by up to 45% under the EXEC scenario and by up to 55% under the MFTR scenario. The models project an increase in air concentrations of GEM between 2005 and 2020 under the SQ scenario, particularly in regions where the highest Hg emissions are expected to occur. These regions include eastern and southern Asia, Europe, and north-western South America. If no major action is taken to reduce current emissions (the SQ scenario) the greatest increase, of up to 20%, is projected for eastern Asia, where most of the emissions occur today. Concentrations of Hg in

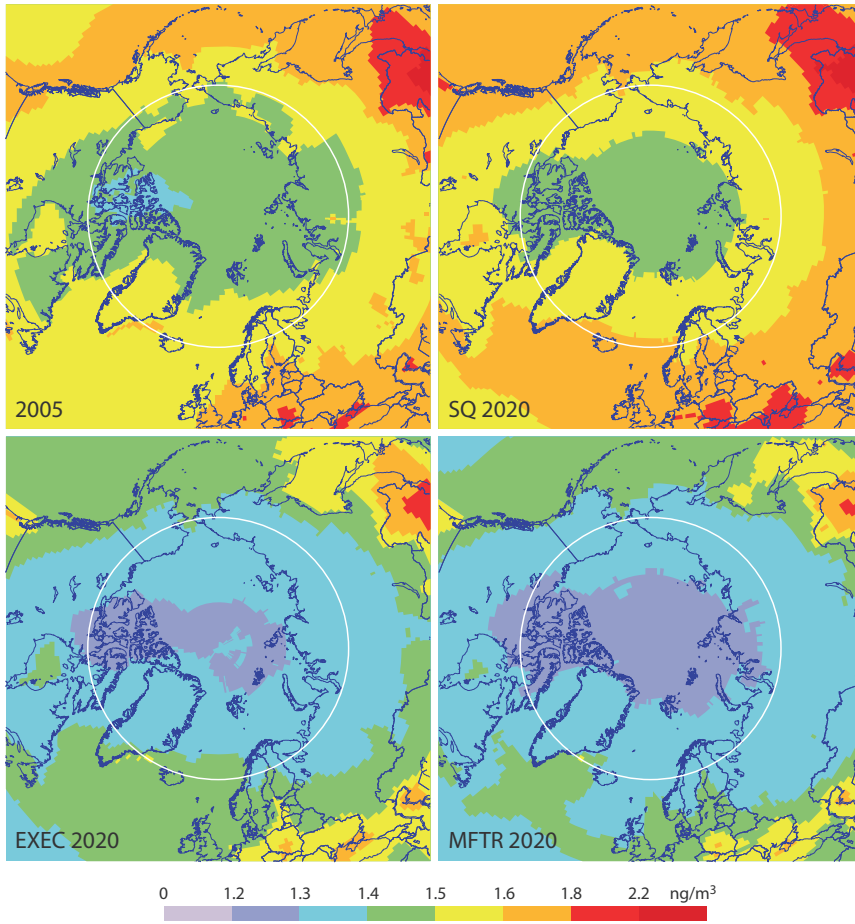


Figure 7.2. Model ensemble average estimate of gaseous elemental mercury concentrations over the Arctic in 2005 and in 2020 under the SQ, EXEC and MFTR emissions scenarios.

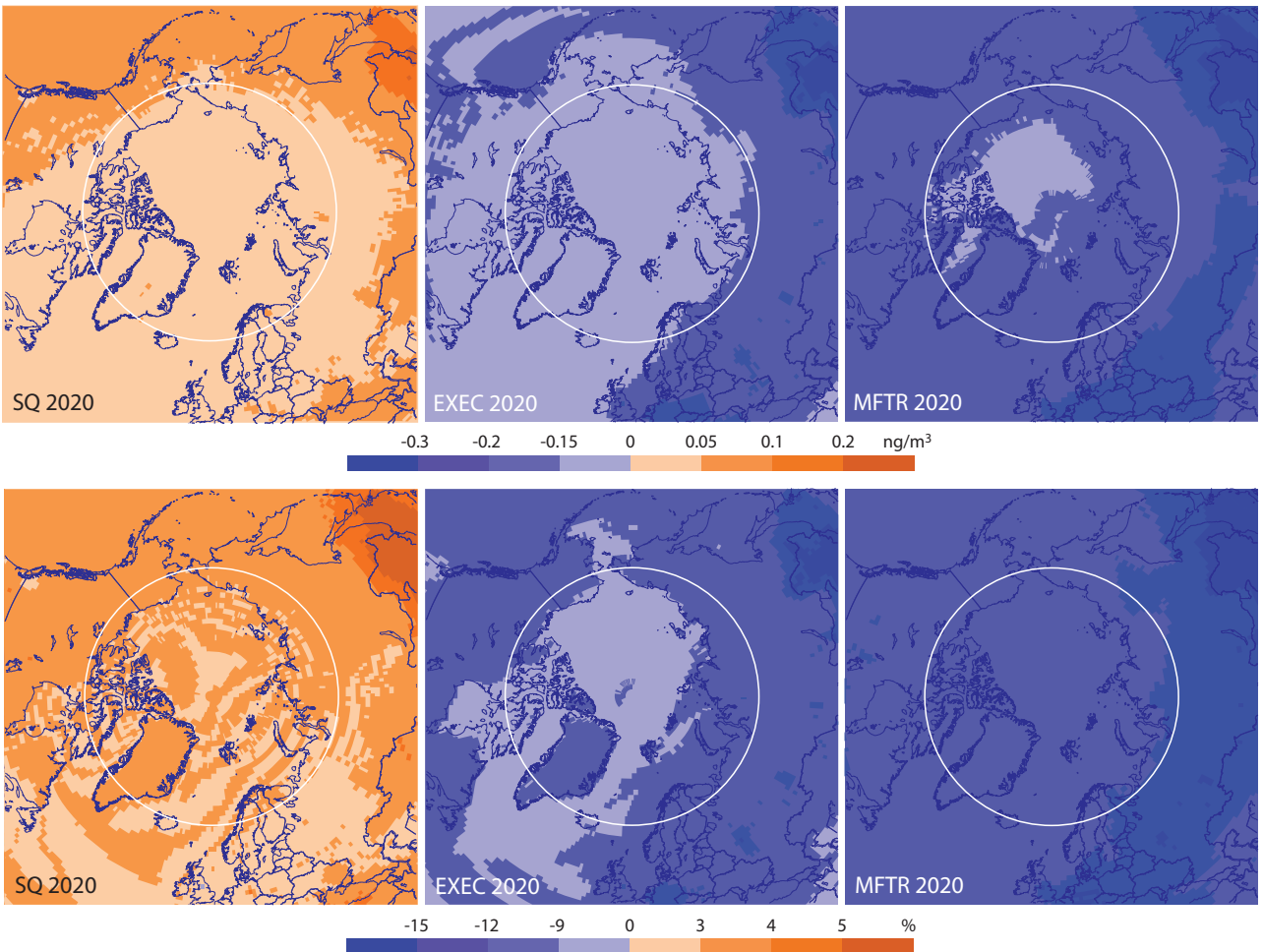


Figure 7.3. Model ensemble average estimate of absolute (above) and relative changes (below) in gaseous elemental mercury concentration over the Arctic between 2005 and 2020 under the SQ, EXEC and MFTR emissions scenarios. Positive values represent an increase.

Table 7.2. Global anthropogenic mercury emissions to air and average atmospheric mercury concentrations for Arctic and sub-Arctic regions in 2005 and as projected for 2020 under the SQ, EXEC and MFTR scenarios.

	Base 2005	SQ 2020	EXEC 2020	MFTR 2020
Global anthropogenic mercury emissions, t	1925	2295	1060	862
	Surface air Hg concentration, ng/m ³			
Arctic 66.5° – 90° N	1.47	1.51	1.34	1.31
European Arctic 10° W – 60° E	1.49	1.54	1.35	1.33
Asian Arctic 60° E – 170° W	1.47	1.51	1.33	1.30
North American Arctic 170° – 10° W	1.46	1.51	1.33	1.31
Sub-Arctic 60° – 66.5° N	1.54	1.59	1.39	1.36
Western European sub-Arctic 10° W – 20° E	1.57	1.62	1.43	1.40
Eastern European sub-Arctic 20° – 60° E	1.56	1.61	1.40	1.37
Western Asian sub-Arctic 60° – 100° E	1.52	1.57	1.36	1.33
Eastern Asian sub-Arctic 100° E – 170° W	1.54	1.59	1.39	1.36
Western North American sub-Arctic 170° – 100° W	1.52	1.58	1.38	1.35
Eastern North American sub-Arctic 100° – 10° W	1.53	1.57	1.39	1.37

air in 2020 are projected to decrease by up to 20% in the most polluting regions of the world under the EXEC scenario and by slightly more under the MFTR scenario.

The model ensemble mean GEM surface air concentrations in the Arctic for 2005 emissions and according to the three future scenarios are presented in Figure 7.2. The spatial variation of the changes (absolute and relative) within the Arctic and sub-Arctic is shown in Figure 7.3. Average air concentrations and percentage change vary for the different regions (see Tables 7.2 and 7.3). Results show an average increase of 3% for the Arctic and 3.1% for the sub-Arctic under the SQ scenario, and an average decrease of 9.1% and 10.9% in the Arctic and 9.6% and 11.5% for the sub-Arctic, under the EXEC and MFTR scenarios, respectively. Variation in the projected change in Hg concentration between different sectors of the Arctic and sub-Arctic is small (SQ: up to 21%, EXEC: up to 19%, MFTR: up to 19%). The increase is greatest in the western North American sub-Arctic under the SQ scenario and the decrease greatest in the eastern European sub-Arctic and western Asian sub-Arctic. These differences are consistent with air flow patterns and the spatial distribution of changes in emissions reported in Section 2.6.1.1.

7.3.2. Projections of atmospheric mercury deposition based on the 2020 emissions scenarios

Estimates of Hg deposition in 2005 and in 2020 according to the SQ, EXEC and MFTR emissions scenarios were modeled using the GRAHM, GLEMOS, and DEHM models. Two types of re-emission terms are considered in the GRAHM model; recent re-emission and legacy re-emission. The re-emission occurring from deposited Hg within the same year is considered as recent and the rest is legacy re-emission from all terrestrial and aquatic surfaces. GLEMOS and DEHM assume no recent re-emission. However, both models are constrained with the measured surface air concentrations and so the deposition could be considered as net deposition. It should be noted that net deposition estimated here is the net Hg being added in a given year to the Arctic environment (gross deposition – quick re-emission of Hg from snow).

The models project an increase in the atmospheric deposition of total Hg by 2020 using the SQ scenario, particularly in eastern and southern Asia, where emissions are projected to increase the most. In the other major source areas most relevant for the Arctic, namely Europe and north-eastern North America, modest rates of increase in emissions are projected. The model

Table 7.3. Change in global anthropogenic mercury emissions to air and mercury concentrations for Arctic and sub-Arctic regions in 2020 under the SQ, EXEC and MFTR scenarios relative to 2005.

	Change, %		
	SQ 2020	EXEC 2020	MFTR 2020
Global anthropogenic mercury emissions	19.2	-44.9	-55.2
Arctic 66.5° – 90° N	3.0	-9.1	-10.9
European Arctic 10° W – 60° E	3.0	-9.3	-11.1
Asian Arctic 60° E – 170° W	3.1	-9.3	-11.1
North American Arctic 170° – 10° W	3.1	-8.8	-10.6
Sub-Arctic 60° – 66.5° N	3.1	-9.6	-11.5
Western European sub-Arctic 10° W – 20° E	2.9	-9.4	-11.3
Eastern European sub-Arctic 20° – 60° E	2.8	-10.5	-12.6
Western Asian sub-Arctic 60° – 100° E	3.1	-10.5	-12.6
Eastern Asian sub-Arctic 100° E – 170° W	3.3	-9.8	-11.8
Western North American sub-Arctic 170° – 100° W	3.4	-9.4	-11.3
Eastern North American sub-Arctic 100° – 10° W	3.0	-8.8	-10.6

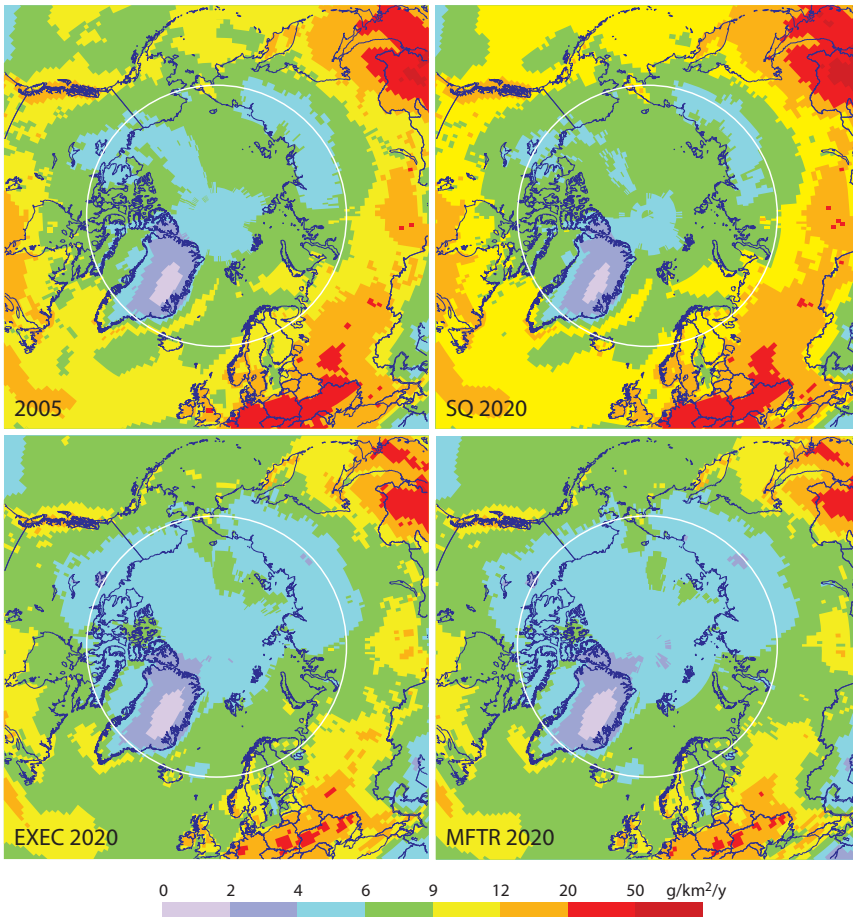


Figure 7.4. Model ensemble average estimate of total mercury deposition over the Arctic in 2005 and in 2020 under the SQ, EXEC and MFTR emissions scenarios.

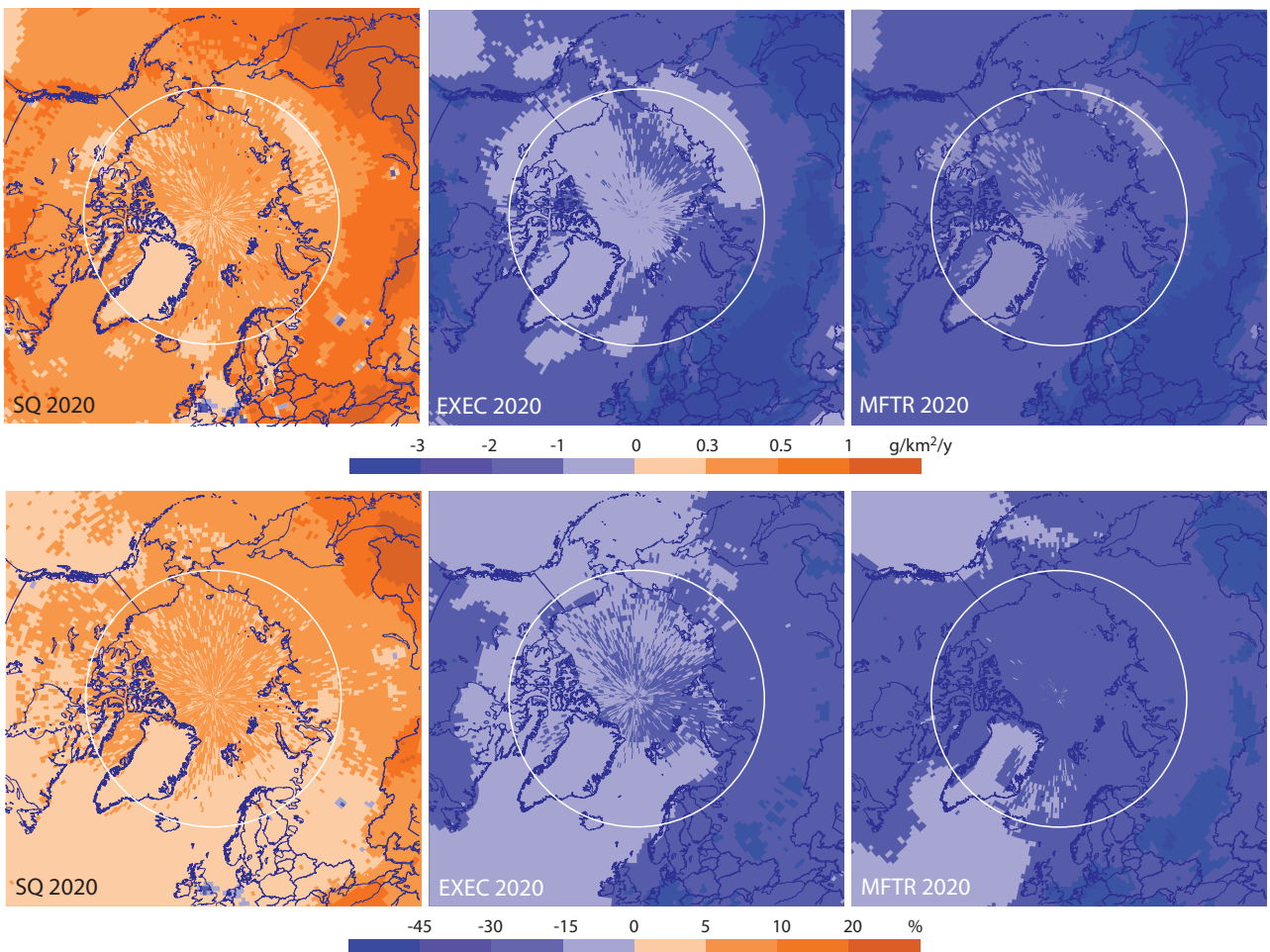


Figure 7.5. Model ensemble average estimate of absolute (above) and relative (below) changes in total mercury deposition over the Arctic between 2005 and 2020 under the SQ, EXEC and MFTR emissions scenarios. Positive values represent an increase.

Table 7.4. Global anthropogenic mercury emissions to air and average total mercury deposition for Arctic and sub-Arctic regions in 2005 and as projected for 2020 under the SQ, EXEC and MFTR emissions scenarios.

	Base 2005	SQ 2020	EXEC 2020	MFTR 2020
Global anthropogenic mercury emissions, t	1925	2295	1060	862
	Hg deposition, $\mu\text{g}/\text{m}^2/\text{y}$			
Arctic 66.5° – 90° N	6.53	6.87	5.56	5.36
European Arctic 10° W – 60° E	8.29	8.66	7.03	6.78
Asian Arctic 60° E – 170° W	6.67	7.03	5.62	5.40
North American Arctic 170° – 10° W	5.67	5.97	4.88	4.72
Sub-Arctic 60° – 66.5° N	8.96	9.39	7.48	7.18
Western European sub-Arctic 10° W – 20° E	10.60	10.99	8.81	8.47
Eastern European sub-Arctic 20° – 60° E	12.40	12.86	9.46	8.90
Western Asian sub-Arctic 60° – 100° E	10.40	10.96	8.30	7.86
Eastern Asian sub-Arctic 100° E – 170° W	7.61	8.06	6.43	6.17
Western North American sub-Arctic 170° – 100° W	7.35	7.73	6.33	6.12
Eastern North American sub-Arctic 100° – 10° W	8.81	9.19	7.71	7.48

results indicate that a significant proportion of the projected increased emissions deposit close to source areas. This may be related to shifts in the speciation of emitted Hg from elemental to divalent forms, as discussed by Streets et al. (2009). Changes in the amounts of elemental Hg between the 2005 and 2020 SQ inventories used in this modeling work are, however, only very modest (of the order of a few percent) compared to particulate and divalent forms of Hg.

The model ensemble mean total Hg deposition (dry and wet deposition) in the Arctic for 2005 and in 2020 according to the three future emissions scenarios is presented in Figure 7.4. The spatial variation of changes (absolute and relative) within the Arctic and sub-Arctic is illustrated in Figure 7.5. Average deposition and percentage change vary for the different regions (see Tables 7.4 and 7.5). Results show an average increase of 5.2% for the Arctic and 4.8% for the sub-Arctic under the SQ scenario, and an average decrease of 14.9% and 18% in the Arctic and 16.5% and 19.9% in the sub-Arctic, under the EXEC and MFTR scenarios, respectively.

A comparison of changes in airborne Hg concentration and deposition reveals that the projected percentage change in deposition is greater than the projected change in air concentration. Furthermore, variations in changes in Hg deposition to the Arctic and sub-Arctic between different

sectors are also greater for deposition than for air concentration (SQ: up to 64%, EXEC: up to 88%, MFTR: up to 87%). These results suggest that the differences in anthropogenic oxidized Hg between the three scenarios affect deposition in the Arctic and sub-Arctic through the direct transport of these species. The stronger variation in changes in deposition can be explained by the gradient in deposition of the directly transported oxidized Hg, regional differences between meteorological factors influencing dry and wet deposition, and differences in upper air concentrations of Hg since wet deposition scavenges Hg at higher altitudes. The impact of changes in remote emissions, such as in Asia, is greater in the free troposphere than in surface air. The projected increase in deposition is found to be somewhat larger for the Arctic than the sub-Arctic, and this could be due to the occurrence of 'atmospheric mercury depletion events' (AMDEs) in the Arctic. Under the SQ scenario, the largest projected regional increase will be in the Asian Arctic and sub-Arctic, followed by the western North American sub-Arctic. The largest projected regional decrease will be in the eastern European sub-Arctic followed by the western Asian sub-Arctic. These differences are consistent with air flow patterns and regional airborne Hg concentrations.

Table 7.5. Changes in global anthropogenic mercury emissions to air and total mercury deposition for Arctic and sub-Arctic regions in 2020 under the SQ, EXEC and MFTR emissions scenarios and relative to 2005.

	Change, %		
	SQ 2020	EXEC 2020	MFTR 2020
Global anthropogenic mercury emissions, t	19.2	-44.9	-55.2
Arctic 66.5° – 90° N	5.2	-14.9	-18.0
European Arctic 10° W – 60° E	4.5	-15.2	-18.2
Asian Arctic 60° E – 170° W	5.5	-15.8	-19.1
North American Arctic 170° – 10° W	5.3	-13.9	-16.8
Sub-Arctic 60° – 66.5° N	4.8	-16.5	-19.9
Western European sub-Arctic 10° W – 20° E	3.6	-17.0	-20.1
Eastern European sub-Arctic 20° – 60° E	3.7	-23.7	-28.2
Western Asian sub-Arctic 60° – 100° E	5.3	-20.2	-24.4
Eastern Asian sub-Arctic 100° E – 170° W	5.9	-15.5	-18.9
Western North American sub-Arctic 170° – 100° W	5.2	-13.8	-16.6
Eastern North American sub-Arctic 100° – 10° W	4.3	-12.6	-15.1

7.3.2.1. Differences in model estimates of changes in net deposition

Figure 7.6 illustrates total net Hg deposition to the Arctic (north of the Arctic Circle) according to the three models (GRAHM, GLEMOS and DEHM). The models estimate total net deposition of Hg to the Arctic to vary within the range ~115 to ~143 t. As discussed in Chapter 2 (Section 2.6.1.2), there are two major sources of uncertainty causing the difference between the model estimates: the halogen chemistry resulting in AMDEs, and global estimates of natural Hg emissions and re-emissions. Under the SQ scenario, deposition is projected to increase by about 10 t in the GRAHM and GLEMOS models while an increase of ~2 t is estimated by DEHM. On the other hand, under the emission reduction scenarios (EXEC and MFTR), the amount of Hg deposited in the Arctic in 2020 is projected to decrease by up to ~40 t (GRAHM), or ~30 t (GLEMOS, DEHM) compared to 2005. The range in projected deposition estimates for the Arctic is presented in Table 7.6. In terms of differences between models, the range is greater for GRAHM than GLEMOS and DEHM, and this can be attributed to higher model resolution in the GRAHM simulations.

Mercury in the Arctic mostly originates from a number of major source areas outside the Arctic (see Figure 7.7). Figure 7.8 illustrates the source attribution of net Hg deposited in the Arctic under the three future emissions scenarios as projected by GRAHM and GLEMOS. Source attribution simulations were not conducted with DEHM. The impact of changing anthropogenic emissions on oceanic and terrestrial re-emissions in the short term was considered in the GLEMOS simulation. Short-term changes in terrestrial and oceanic re-emissions (within a few years) are minimal under the scenarios considered; it is expected that over the long term, changes in anthropogenic emissions will lead to further changes in terrestrial and oceanic re-emissions. Eastern Asia is seen to be a major source region with the greatest potential for emission reduction and thus for reduction of Hg deposition in the Arctic. The GRAHM and GLEMOS models indicate that as much as 22 to 25 t of Hg will be deposited to the Arctic from anthropogenic emission sources in eastern Asia if the SQ scenario is maintained. Alternatively, under EXEC and MFTR the deposited emissions will be reduced by 13 to 17 t from eastern Asia alone. Relative changes in anthropogenic

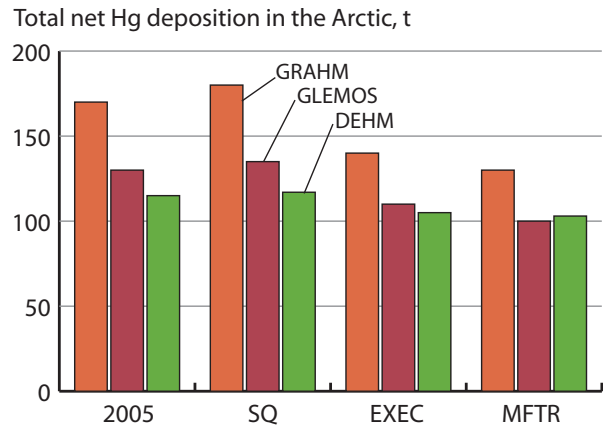


Figure 7.6. Total net mercury deposition in the Arctic (north of the Arctic Circle) according to the GRAHM, GLEMOS and DEHM models, for 2005 and as projected for 2020 under the SQ, EXEC and MFTR emissions scenarios.

emissions in the source regions lead to corresponding changes in source attribution of net Hg deposition in the Arctic. Figure 7.8 also illustrates that a large proportion of the Hg that ends up in the Arctic is carried in via ocean currents.

The GRAHM and GLEMOS models agree with respect to the contribution to deposition in the Arctic from anthropogenic sources, but differ with respect to the contribution from natural sources and re-emissions in the major source regions (Figure 7.8). Re-emissions in Europe, North America and eastern Asia are significantly higher in GRAHM compared to GLEMOS and this results in a larger overall deposition contribution simulated by GRAHM from these regions to the Arctic.

In summary, the models agree well in terms of their projected changes in net deposition (Figure 7.6), as well as their projected changes in source attribution. Changes in the relative contributions of the source regions to net Hg deposition in the Arctic, increase or decrease consistent with changes in anthropogenic emissions in these regions. Given that a significant proportion of the Hg being deposited in the Arctic is from the re-emission of previously deposited Hg, more studies are required for quantitative and mechanistic understanding of the long-term impact of changes in anthropogenic emissions on re-emissions from soils, water and vegetation.

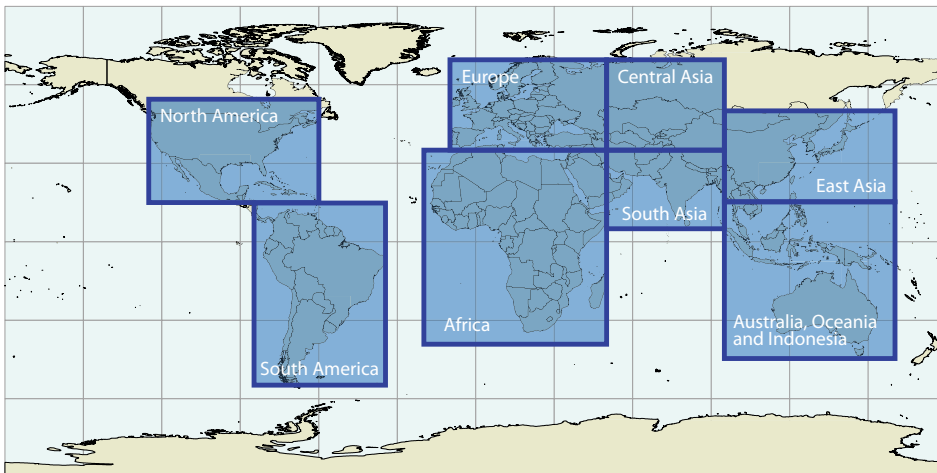


Figure 7.7. Major source regions for atmospheric mercury in the Arctic.

Table 7.6. Range in total net mercury deposition projected for the Arctic.

Total net Hg deposition Baseline (2005)	GRAHM		GLEMOS		DEHM	
	2 to 12 g/km ² /y		0 to 9 g/km ² /y		1 to 12 g/km ² /y	
Change in net deposition	Absolute, g/km ² /y	Relative, %	Absolute, g/km ² /y	Relative, %	Absolute, g/km ² /y	Relative, %
SQ	0 to 0.5	0 to 15	0 to 1	3 to 5	0 to 0.5	0 to 5
EXEC	-0.5 to -5	-5 to -30	0 to -2	-10 to <-30	0 to -2	0 to -15
MFTR	-0.5 to -5	-5 to -30	0 to -2	-15 to <-30	0 to -2	0 to -15

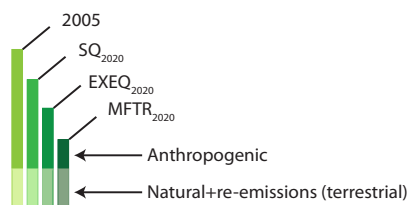
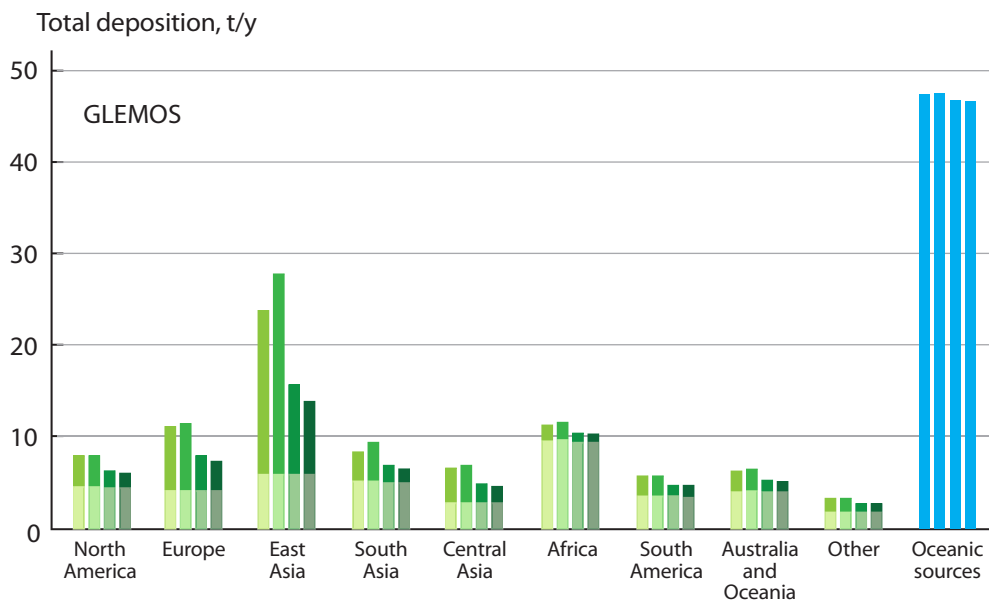
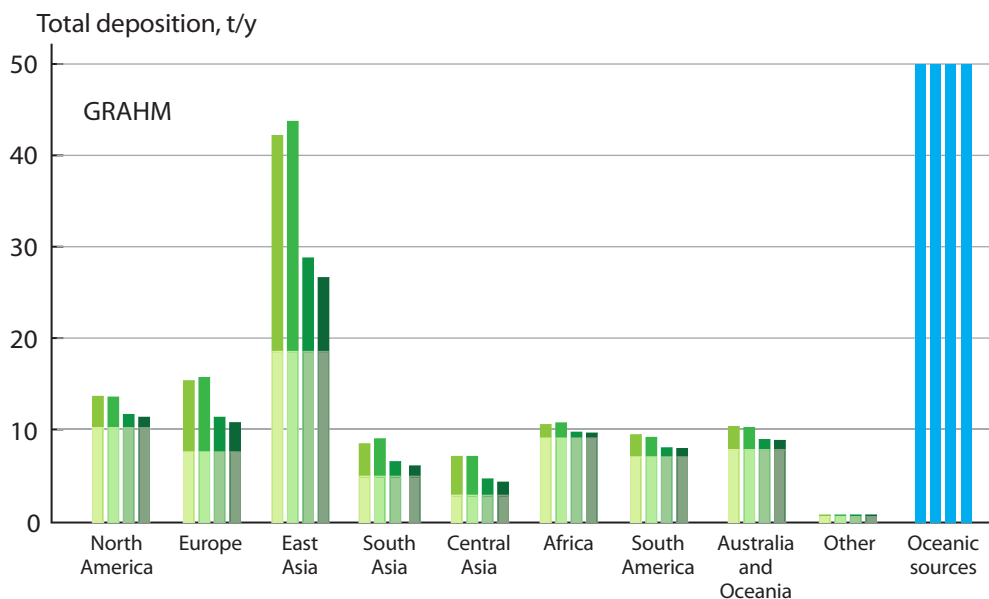


Figure 7.8. Net mercury deposition to the Arctic as modelled by GRAHM (above) and GLEMOS (below) for 2005 and 2020 according to the three future emissions scenarios, showing the relative contribution from anthropogenic emissions, terrestrial natural and re-emitted mercury from the major source regions, and the global ocean.

7.3.3. Projections of change in mercury deposition with changing climate

To compare the relative effects of changes in global emissions on airborne Hg deposition in the Arctic against those from future climate changes, two different modeling exercises were undertaken. First, the GRAHM model was used to investigate the effects of meteorological variations on atmospheric Hg deposition in the Arctic. Preliminary results for temporal changes in GEM surface air concentrations at Alert, Canada are shown in Figure 7.9. Concentrations during October to December represent background levels and the model estimates represent average concentrations in the region around the measurement site. Comparison of model output with measured concentration data suggests that interannual variability in meteorology is partly responsible for the year-to-year variation in GEM observed at Alert. The modeling results also suggest that the decrease in surface air GEM concentrations between 1995 and 2000 and the subsequent increase between 2000 and 2005 is primarily due to changes in global anthropogenic emissions. The model has not yet been used to examine temporal trends in air concentration and deposition across the Arctic as a whole. Changes in natural emissions and re-emissions are not considered.

In a second exercise, the DEHM model was used to examine the effects of climate change on future projections of Hg deposition in the Arctic. Emissions were kept at the 2005 level and meteorological data from ECHAM5/MPI-OM were used. Two historic decades were simulated (1890-1899 and 1990-1999) along with two future decades (2090-2099 and 2190-2199) with the meteorology from the same scenario (IPCC A1B scenario) for consistency between simulations. One of the weaknesses of such simulations is that the parameterizations of some processes may not be adequate to represent the changing environmental conditions. Uncertainties in the model projections can be reduced by using an ensemble of models rather than estimates from a single model. However, at present climate impact simulations from other models are not available. By comparing mean values for a decade with variations in the yearly values within the decade, it is possible to establish whether the difference between decades is significant compared to the year-to-year variation. Figure 7.10 compares

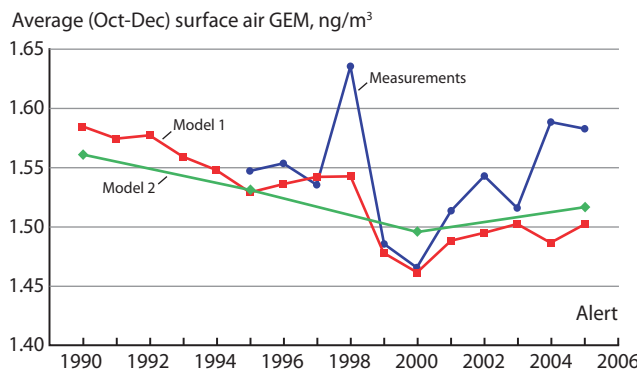


Figure 7.9. Average (October–December) surface air GEM concentrations at Alert, Canada between 1995 and 2005. The graphic compares measured concentrations with two sets of output from the GRAHM model: one which includes changing meteorological conditions and one with conditions kept constant. Source: data from A. Steffen, pers. comm.

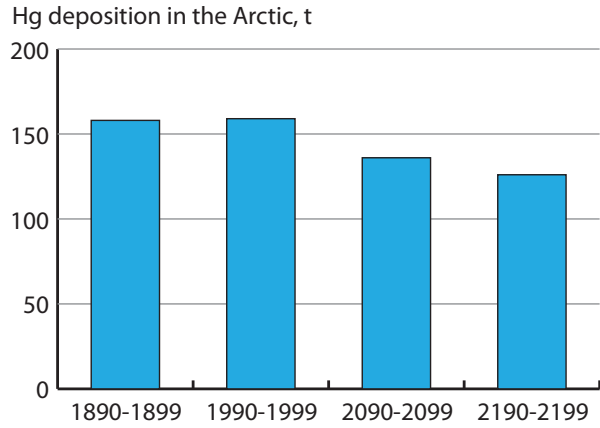


Figure 7.10. Mean mercury deposition in the Arctic for two historic decades (1890-1899 and 1990-1999) and two future decades (2090-2099 and 2190-2199) as modeled by DEHM.

the differences between total Hg deposition for the area north of the Arctic Circle for each of the four decades. The results show minimal differences between the 1890s and 1990s but a significant decrease from the 1990s to 2190s. Figure 7.11 compares yearly mean deposition of total Hg for the 1990s and 2190s. The results show a significant decrease in Hg deposition over the Arctic Ocean and a significant increase over the continents. The main reason for the decrease over the Arctic Ocean is the change in ice cover, and its influence on AMDEs in the DEHM model. The main reason for the increase in deposition over the continents is a significant increase in ozone concentrations in the troposphere; ozone is the main oxidant of Hg in the DEHM model.

7.4. What will be the recovery time for mercury in the Arctic atmosphere and ocean under future scenarios of emissions reductions?

7.4.1. Recovery time of the Arctic atmosphere

If the negotiations currently underway to establish a global agreement on Hg under the auspices of UNEP are successful, it can be expected that there will be an increased impetus in the adoption of measures to reduce emissions of Hg in the coming years, beyond those that are already planned in some countries.

In the work presented in Section 7.3, the SQ scenario represents, if not a worst case scenario, then certainly a pessimistic scenario for developments up to 2020, with increased emissions driven by continuing economic growth in the absence of new control measures. Conversely, while the MFTR scenario is unrealistic because it is not constrained by costs associated with implementing control technologies, and it is highly unlikely that some of the more ambitious control technologies assumed could be introduced worldwide within the next ten years, it could be considered a qualified best-case scenario. It should also be remembered that the SQ and MFTR scenarios only consider changes in emissions from ‘by-product’ source sectors (see Section 2.2), and not emissions associated with intentional-use sectors. The latter are very difficult to project into the future and thus are treated as unchanged

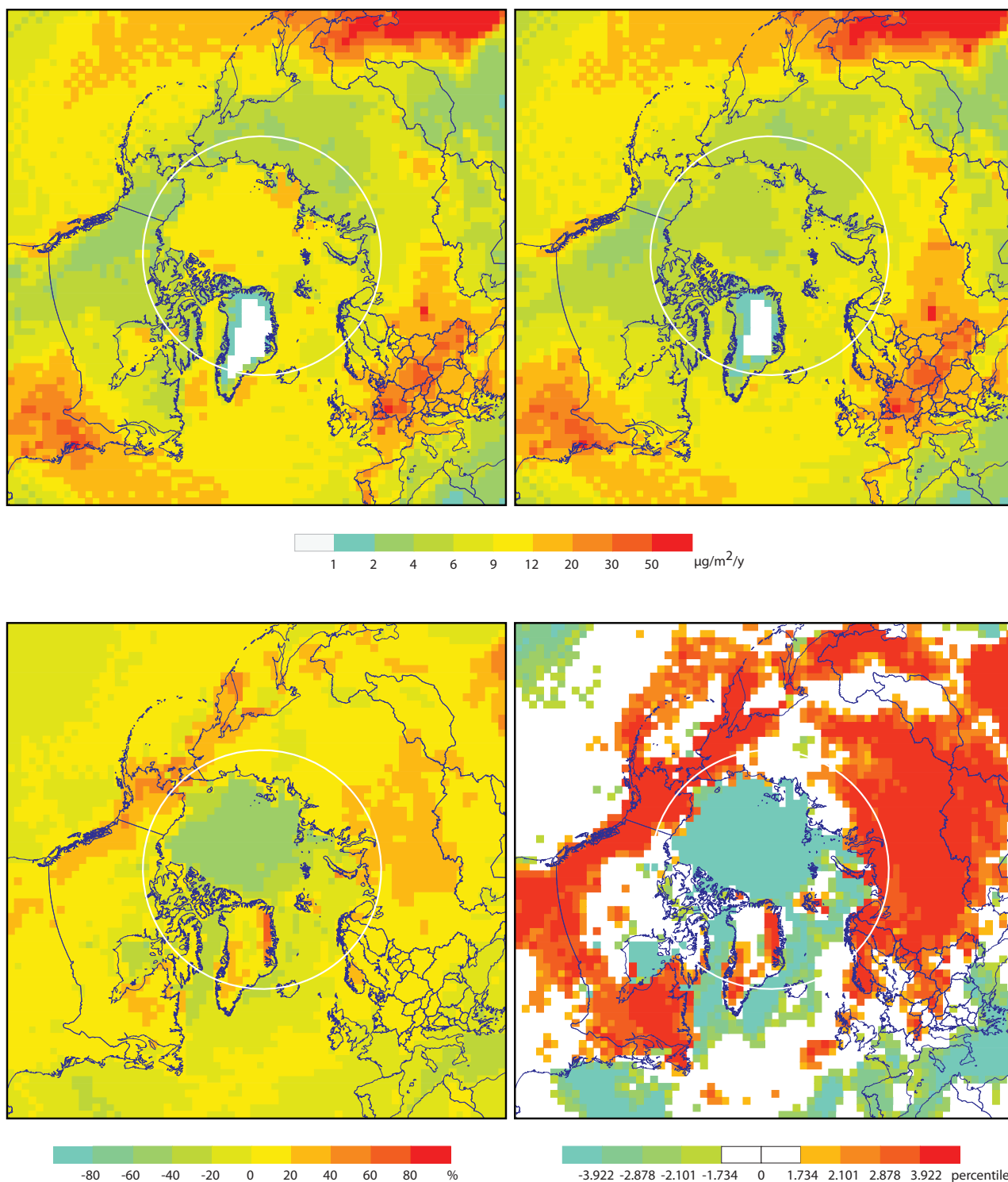


Figure 7.11. Yearly mean deposition of total mercury for 1990-1999 (upper left) and for 2190-2199 (upper right), the percentage difference (lower left) and the t-test (lower right). The t-test legend corresponds to differences that are significant at $p < 0.10$, 0.05, 0.01 and 0.001.

relative to 2005 in the modeling applications described in the previous section. There is potential for further reductions in emissions beyond the MFTR scenario if, for example some major (intentional-use) emission sources, such as artisanal and small-scale gold mining (which accounts for some 350 t/y of Hg emissions) could be restrained. Also, emissions from crematoria may decrease (with some time lag) as Hg use in dentistry is phased out. However, there are also potential

increases in emissions as, for example, Hg in products currently circulating in society enters the waste stream.

With this in mind, and also considering the uncertainties associated with models, the modeling presented in the previous section using the MFTR scenarios can be used to provide some indication of ecosystem recovery following emissions reductions. Some possible conclusions are as follows:

- Comparing projections for 2020 against 2005, the total (net) Hg deposition within the Arctic is reduced by some 15 to 50 t (DEHM and GRAHM models), compared with the estimates of total net deposition in 2005 of around 120 to 170 t by these models. Both model outputs, it should be noted, are highly dependent upon accurate AMDE characterization.
- The major effect of the emissions reductions under the MFTR (and EXEC) scenarios are projected to occur in the major source regions (in particular south-eastern Asia). This is likely to reflect the effective control of emissions of particulate and Hg(II) forms that tend to deposit closer to the source areas. The relatively modest reduction of deposition projected for the Arctic is due to moderate decreases in the deposition associated with long-range transport (mainly GEM) to the region.
- The direct response of the Arctic atmosphere to changes in Hg emissions, although modest, can be expected to be relatively fast, reflecting the short atmospheric lifetime of in particular particle-associated and reactive Hg(II) species; GEM has a somewhat longer lifetime in air (about 6 to 24 months).
- There will also be an indirect effect on the atmosphere due to Hg re-emissions from surfaces and environmental reservoirs such as soils and oceans. These add considerable inertia in the system, and load up the atmosphere for a considerable period even if future anthropogenic emissions cease or are strongly reduced. Nevertheless, it is important to remember that reduction in atmospheric emissions (and direct discharges of Hg to aquatic environments) are the essential first step in decreasing the environmental pools of Hg in other compartments.
- Extending modeling projections using the MFTR scenario for longer periods into the future (e.g., to 2050 or 2100) might be one way to investigate the response of the atmosphere to re-cycling of Hg following emissions reductions.
- The atmospheric signal from emissions reductions is stronger close to the major source areas than it is in remote areas because the former are also impacted to a greater extent by deposition of Hg emitted in divalent and particulate-associated species. This is likely to be part of the explanation as to why trends in environmental media close to source areas appear to reflect emissions trends better than those in remote areas, where the trend component from changes in anthropogenic emissions/deposition will be smaller and possibly subjugated by other factors that may determine overall trends, such as changes in food-web structures or climate influence on environmental pathways.
- Changes in Hg loadings in other environmental compartments, including biota and food webs – representing chemical and biological recovery under assumed emissions reduction scenarios – will occur at slower rates, with response times determined by processes that affect environmental Hg cycling. The environmental reservoirs of Hg (in particular in soils and oceans) are larger than they were in the pre-industrial period. For this reason, in the absence of other factors (such as climate change) rates of ‘recovery’ (i.e., decreasing environmental Hg concentrations) following emissions reductions would be expected to be slower than the rates of ‘deterioration’ (i.e., increasing environmental Hg concentrations) that occurred as Hg emissions increased following the pre-industrial period. Put another way, the associated lag times in environmental response to changes in emissions are likely to be longer on the way down than they were on the way up.
- All the modeling and scenario-based discussion presented above relates only to controls applied to primary anthropogenic emission to the air. Chapter 4 of this assessment clearly illustrates that climate change will have major influences on contaminant transport pathways and environmental recycling, that could easily act to mask any more intuitive changes in atmospheric Hg concentrations and deposition associated with emissions reductions. It is also likely to have major influences on Arctic ecosystems (in particular marine ecosystems) that will influence apparent biological recovery from emissions reductions. Finally, climate change in itself is likely to impact Hg emissions in the future through, for example, changing patterns of fuel use.
- Assessing the impact of climate change on environmental and ecosystem recovery is a major challenge that is only now beginning to be addressed through, for example, modeling investigations. This represents a likely (and much needed) focus for future research and modeling activities, introducing new demands for coupled multi-compartment models.

7.4.2. Recovery time of the Arctic Ocean

Atmospheric inputs are just one of a number of significant pathways for Hg to enter the Arctic Ocean and which control Hg dynamics in Arctic seawater (Outridge et al., 2008). Estimation of the ocean’s response to changing global emissions therefore requires: (i) an understanding of the extent to which present-day Hg levels in the ocean are controlled by atmospheric inputs, (ii) the assumption that all of the other inputs/outputs in the ocean will not change significantly as a result of either direct human impacts on the Arctic Hg cycle, or from the effects of future climate warming. As Outridge et al. (2008) pointed out, current understanding of the marine Hg cycle, especially in the Arctic, is insufficient to make this estimation with a great deal of confidence.

7.4.2.1. An updated box-model of mercury in the Arctic Ocean

To provide a basis for estimating the impact of future changes in emissions on Hg levels in Arctic Ocean seawater, the box-model for total Hg in the Arctic Ocean recently constructed by Outridge et al. (2008) (see Section 2.4), was adapted. The latter authors developed the model by referring to published literature for estimates of physical exchanges between the Arctic Ocean and the Pacific and Atlantic Oceans, ice export from the Arctic Ocean, river inflow (particulate and dissolved), coastal erosion (particulate), precipitation and sedimentation. To calculate the Hg flux, all media were assigned plausible Hg concentrations based on literature values from the Arctic or elsewhere (see Table 3 in Outridge et al., 2008). Atmospheric net deposition of Hg to the surface of the Arctic Ocean, which is difficult to estimate directly as there are few suitable measurements, was

estimated from a modified GRAHM model. Comparing the inventory of Hg in the Arctic Ocean with the fluxes of Hg from the sources or to the sinks, these authors proposed that Hg had a relatively short residence time (about five years) in the top 200 m of the Arctic Ocean, which suggests that surface waters would respond on about that time scale to changes in Hg fluxes into or out of the Arctic. The Outridge et al. model synthesized a great deal of information from many sources, and found that inputs and outputs of Hg are close to being in balance at present. However, from the perspective of understanding how the Arctic Ocean might respond to proposed changes in atmospheric emission/deposition (or any other input/output parameter), the published model has one shortcoming in that it considers the Arctic Ocean to be a single sea (one box for less than 200 m depth, one box for deeper water).

A particularly important feature of the Arctic Ocean is that its surface waters comprise two distinct domains (see Figures 7.12 and 7.13) (Macdonald and Bowers, 1996), and so this ocean could realistically be considered as two oceans. The distinct domains in Arctic Ocean surface waters have important implications for understanding the distributions and trends of contaminants (e.g., see the contrasting distributions for HCH and radionuclides reported by Carmack et al., 1997; their Figure 6). The eastern Arctic surface water, which communicates predominantly with the Atlantic Ocean, is the terminus for European and North American contaminants following either ocean currents (Gobeil et al., 2001a), or storm tracks leading northward approximately along the prime meridian (Macdonald et al., 2005). In contrast, the western Arctic Ocean receives via Bering Strait an inflow of low-density seawater from the Pacific Ocean, which then rides over the denser Atlantic water and provides the dominant source for western Arctic Ocean surface waters (Figure 7.13). Oceanic and atmospheric transport pathways for the western Arctic therefore favor Asian

contaminant sources (e.g., Li et al., 2002, 2004). Within the Arctic Ocean, the two domains are distinguished by a large clockwise eddy in the west (the Beaufort Gyre), and a rapid surface transport (the Transpolar Drift) across the center of the Arctic Ocean roughly aligned with the Lomonosov or Alpha-Mendeleev Ridges (McLaughlin et al., 1996).

Given that the Hg emissions and transport pathways to the Arctic are very different for Europe / North America and Asia, it seems certain that western and eastern Arctic surface waters have responded differently to historical contaminant Hg exposures and will respond differently in the future to whatever emission controls are put in place. The perspective of distinct east-west contaminant domains in the Arctic Ocean may provide part of the answer as to why Hg trends and concentrations in top marine predators appear to differ between these two regions (see Chapter 5).

To revise the Outridge et al. (2008) budget, the Arctic Ocean has been divided into two domains using Stein and Macdonald (2004) to apportion areas and water volumes for shelves and basins (see Figure 7.12). The western Arctic domain has been assigned the shelves north of the Archipelago, the Beaufort and Chukchi Shelves and the eastern half of the East Siberian Shelf, which is dominated by Pacific water (e.g., Semiletov et al., 2005). For this budget, only the upper 200 m of the Arctic Ocean is considered, since this is where the consequences of atmospheric deposition are most immediate and important, and where most of the biological activity occurs. The same methods as outlined in Outridge et al. (2008) are followed, with the exception that (i) fluxes and inventories are partitioned into western and eastern Arctic Ocean basins (Figures 7.12 and 7.13); (ii) particulate and dissolved Hg inputs and outputs are distinguished; (iii) a term for upwelling is specifically included; and, (iv) the Hg budget is balanced, although this need not necessarily be true at present. The Hg budget itself rests on



Figure 7.12. A schematic illustration showing the Arctic Ocean to consist of two major domains roughly separated by the Lomonosov or Alpha-Mendeleev Ridges. The western Arctic Ocean, which is dominated by the Beaufort Gyre, receives input from the Pacific Ocean and supports most of the outflow through the Canadian Arctic Archipelago. The eastern Arctic Ocean is strongly connected with the Atlantic Ocean via Fram Strait and the Barents Sea. It is dominated by the Transpolar Drift. Source: Macdonald and Bowers (1996).

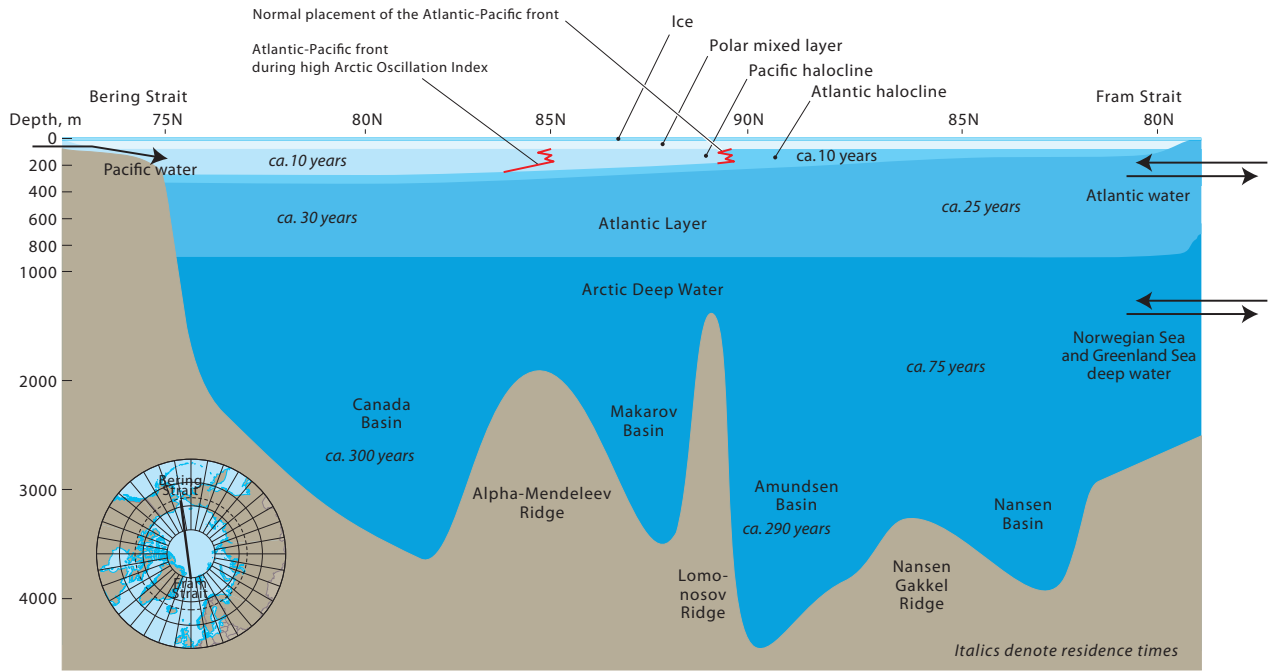


Figure 7.13. A cross section of the Arctic Ocean from Bering Strait, across the North Pole and out through Fram Strait. The upper ocean is shown to consist of two domains, one dominated by water of Pacific origin, the other of Atlantic origin. The surface water is separated from deeper water by pervasive haloclines. Source: Macdonald and Bowers (1996).

balanced budgets for seawater exchange (volumetric flows) and sediments (mass fluxes) within each basin and for the entire Arctic Ocean based on literature compilations (e.g., Rudels and Friedrich, 2000; Stein and Macdonald, 2004; Serreze et al., 2006). Using the balanced water and sediment budgets, the Hg budget is then balanced by minor adjustments of selected Hg concentrations in the various transporting media from those tabulated by Outridge et al. (2008).

In the revised budget (Figure 7.14 and Table 7.7), fluxes involving dissolved aquatic Hg are shown as open arrows while particulate fluxes are in black. In both basins, the atmospheric deposition term is a key term while river contributions of dissolved Hg tend to be relatively small, as is Hg associated with ice export and upwelling. Note that for the purposes of this budget, it is assumed that the net flux of atmospheric Hg is deposited as particulate Hg(II) to the surface but

immediately enters the dissolved Hg(II) pool in the ocean. In the western Arctic, Hg entering from atmospheric deposition, and to a minor extent Pacific inflow, are balanced by almost equivalent fluxes of Hg into shelf sediments and out through the Archipelago. The important finding here is that of the 47 t/y of dissolved Hg entering the western Arctic Ocean, almost half becomes scavenged by particles and buried mostly in shelf sediments along with part of the imported particulate Hg, together making up 25 t/y. A small component is exported in the particle flux to the deep ocean. In the eastern Arctic Ocean, atmospheric deposition is also important, but exchange with the Atlantic Ocean clearly cannot be neglected. The flux of Hg associated with the East Greenland Current is partly a consequence of the size of the current and partly due to the Hg concentration assumed for this water. Again, mirroring the western Arctic Ocean, of the 96 t/y of dissolved Hg entering the

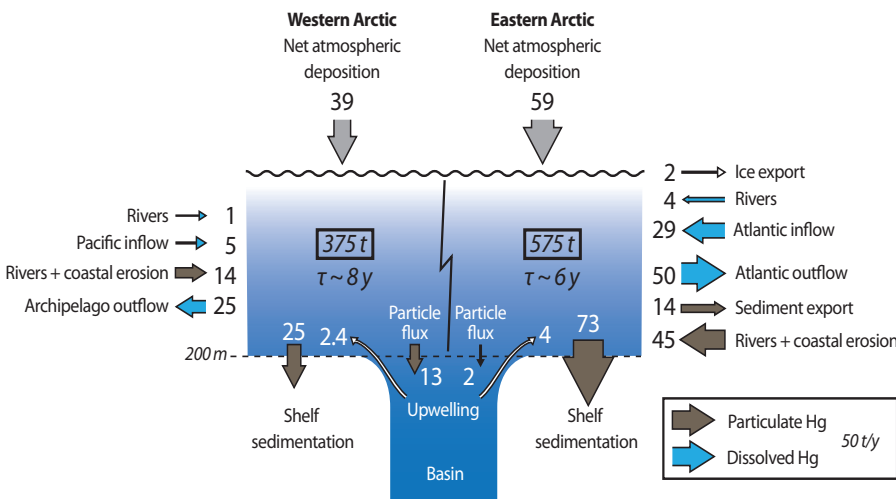


Figure 7.14. A schematic box model showing the mercury budget for the two-domain Arctic Ocean model in circa 2005. The budget is constructed for a Pacific domain (western Arctic) and an Atlantic domain (eastern Arctic) as shown in Figures 7.12 and 7.13.

Atmospheric mercury fluxes include additions to the ocean from wet and dry deposition of reactive gaseous mercury and particulate mercury, and losses through re-emission and evasion of gaseous elemental mercury. A net deposition estimate incorporating the AMDE effect on wet and dry deposition, as well as re-emission from snowpacks and evasion from the ocean, was determined using a modified GRAHM model.

Table 7.7. Elements of the two-domain mercury mass budget for the Arctic Ocean (see Figure 7.14). Source: adapted from Outridge et al. (2008).

	Western Arctic		Eastern Arctic		Whole Arctic	
	Inputs, t/y	Outputs, t/y	Inputs, t/y	Outputs, t/y	Inputs, t/y	Outputs, t/y
Inventory, t	375		575		950	
Atmospheric deposition	38.6		59.4		98.0	
Pacific inflow	5.0		29.3		34.4	
River inflow	0.9		3.7		4.6	
Upwelling	2.4		4.3		6.7	
Sediment influx	14.0		45.1		59.2	
Archipelago outflow		24.6		50.4		75.0
Shelf sedimentation		25.0		73.0		98.0
Basin sedimentation		12.6		2.1		14.7
				14.4		14.4
				1.8		1.8
Dissolved	47.0	24.6	96.7	52.1	143.7	89.7
Particulate	14.0	37.6	45.1	75.1	59.2	114.1
Total balance	61.0	62.2	141.8	141.6	202.9	203.8
Residence time, t/y	8.0		5.9		6.6	
k, 1/y	0.13		0.17		0.15	

Eastern Arctic Ocean about 44 t/y – or half – is buried in shelf sediments together with Hg on particles from coastal erosion and riverine sources. Particle flux of Hg into basin waters is low and probably occurs predominantly as leakage of terrigenous particles at the shelf edge via resuspension over the slopes (e.g., O'Brien et al., 2006). The interior basins of the Arctic Ocean have low productivity and very low associated particle fluxes (Hargrave et al., 1994; O'Brien et al., 2006), which are estimated to support a Hg flux of < 1 t/y. The balance of the 15 t/y lost to basins is made up from resuspended material advected laterally from continental shelves. An interesting implication of the budget in Figure 7.14 is, therefore, that Hg is scavenged over the shelves by the large supply of terrigenous and marine particles whereas waters in the interior ocean have a very weak particle scavenging and flux potential and so are unable to lose Hg, except by exchange of seawater. The result of this large-scale distribution of scavenging would then lead to generally higher dissolved Hg concentrations in the interior ocean relative to the shelves which might then help to explain biogeographic domains in Hg observed in zooplankton of the western Arctic (Stern and Macdonald, 2005) and higher concentrations of Hg in beluga feeding offshore compared to those feeding in the estuary/shelf region of the Beaufort Sea (Loseto et al., 2008b).

7.4.2.2. Response time of mercury in the Arctic Ocean

The time required for the Arctic Ocean to respond to changes in the magnitude of Hg sources can be considered in two ways. First, as a conservative estimate of the Arctic Ocean's ability to adjust to changes in contaminant loading, the natural time scales for replacing the ocean water or ice within the Arctic Ocean are considered. Arctic Ocean surface waters have an

estimated flushing time of about 10 years, where flushing time is the inventory of meteoric freshwater in the ocean divided by the inflow of freshwater from land and by precipitation (Östlund, 1982). The shelves themselves have freshwater flushing times of < 1 year for the Beaufort Sea to 3.5 years for the large Siberian shelves (Macdonald, 2000). These residence times correspond to half-lives of up to 2.5 years for shelf waters and about 7 years for Arctic Ocean surface waters. Therefore, change in an input parameter, like deposition from the atmosphere, will take up to 35 years (5 half-lives) to fully manifest the change in water concentrations. Sea ice in the Arctic Ocean comprises first year ice, which melts out every summer, and multi-year ice, which survives at least one summer. For seasonal ice, Hg deposited to the ice surface in winter and spring is lost to the water during summer and only a seasonal build-up is possible. The memory of first-year ice for contaminant deposition is therefore less than a year and first-year ice-associated food webs might be expected to respond to changes in annual deposition. Although multi-year ice survives the summer, it goes through ablation during the warm period and then new ice is formed on the bottom during the subsequent winter such that the ice will lose a proportion of deposited Hg but then accumulate new Hg during the frozen season (e.g., see Macdonald et al., 2005, their Figure 17, and Stern and Macdonald, 2005). Ice drift tracks and speeds within the permanent pack follow the large-scale surface transport patterns set by the Beaufort Gyre and the Transpolar Drift (see Macdonald et al., 2005, their Figures 14 and 15). If multi-year ice is formed in the Beaufort Gyre, it may take up to 7 years before drifting out of the Arctic via Fram Strait, but less than 2 years if it is formed in the Transpolar Drift. Therefore, the memory of contaminant deposition on ice within the Arctic Ocean is less than 1 year for seasonal ice and up to 7 years for multi-year ice. Ice does not survive transport

through the Archipelago, although its melt products may and, therefore, ice exiting the Arctic Ocean into the Archipelago will yield its Hg burden to the water during transit.

In the box model (Figure 7.14), the inventories (375 t, 575 t, and 950 t for the eastern, western and whole Arctic Ocean, respectively) divided by respective dissolved Hg input components imply residence times for Hg of 8 years in the west and 6 years in the east. These values are highly plausible when compared to the flushing times: they imply that Hg is not conservative (i.e., there are losses within the two domains) and that replacement of water in the western Arctic is slightly slower than in the eastern Arctic, which is also reasonable given the contrast of storage of water within the Beaufort Gyre versus rapid transport by the Transpolar Drift. The box-model budget now makes it possible to ask specifically how the surface water of the Arctic Ocean (western and eastern) would respond to changes in atmospheric Hg deposition. The simplest approach is to proceed based on the scenarios proposed in Section 7.3 for atmospheric deposition. Specifically, it is assumed that in response to the emissions control scenarios it will take 15 years for atmospheric deposition of Hg in the Arctic to be reduced by 5-20% from the 2005 levels. Using the box model, the atmospheric deposition term in the eastern and western Arctic Ocean boxes is reduced linearly between 2005 and 2020. Starting with the 2005 ocean Hg inventories (375 t western, 575 t eastern), the inventories are recalculated annually by summing the new inputs and outputs reflecting change in atmospheric deposition. In this type of model, the reduction in inventories directly implies a parallel reduction in total Hg concentration in the water. Therefore, it is also assumed that fluxes out of the Arctic, including Archipelago and Atlantic outflows, ice export and shelf/basin sedimentation scale linearly with the inventories/concentrations. It is further assumed that other Hg inputs (river inflow, Atlantic and Pacific inflow) remain constant over the time period in question.

Following this procedure it is apparent that for a 5% reduction in atmospheric deposition between 2005 and 2020, Arctic Ocean surface water inventories are reduced by 2.4% in the west and 2.1% in the east by 2020. Likewise, a 20% reduction between 2005 and 2020 corresponds to reductions of 9.5% in the west and 8.3% in the east. If it is assumed that the atmospheric deposition stabilizes after 2020, by 2050 the reductions resulting from the 5% and 20% scenarios will be 4.2% and 16.4% in the west compared to 8.3% and 12.1% in the east. At first, these results seem surprising, and contrary to the longer residence time for Hg in the western Arctic Ocean. However, in the eastern Arctic Ocean, the atmospheric input is accompanied by large input from the Atlantic Ocean such that a given percentage reduction in deposition becomes a smaller percentage reduction in the total Hg input. If it is assumed that Atlantic inflowing water undergoes a reduction in Hg scaled to the lower atmospheric deposition, the eastern basin response becomes slightly faster than the western basin, as would be expected. However, this brings up an important consideration of how the global upper ocean is likely to respond to reductions in Hg emissions. Sunderland and Mason (2007) proposed that the anthropogenic Hg enrichment of the surface ocean is a mere 25% compared to 300-500% in the atmosphere. If this is applicable to the North Atlantic and Pacific Oceans, then the prospects of altering the input of Hg via Fram Strait, the

Barents Sea and the Bering Strait inflows would seem to be minor and take time (the upper global ocean has a Hg residence time estimated at ~70 years). These circumstances are clearly different to those for HCH (Li et al., 2004) and DDT (Stemmler and Lammel, 2009).

The box model also has other implications. The river inflows of dissolved Hg provide only a small part of the budgets, which implies that changes in river inflow or Hg concentration in river waters are likely to have only local (estuarine/shelf) impacts. Likewise, the Hg inflow from the Pacific is estimated to be small, but there are no Hg data for Bering Strait seawater that could provide a confident estimate of present flux. If Hg concentrations at Bering Strait were higher, similar to those in the North Atlantic Ocean (i.e., ~0.3 ng/L), the influx could be as much as 15 t/y, which then becomes a significant component of the western Arctic Ocean budget. Climate variability and change can affect the parameters in this box model. Of all the parameters, the net atmospheric deposition would seem to offer the greatest potential for change given that ice cover has undergone large and rapid change during the past decade, and the Arctic Ocean is projected to be clear of ice seasonally possibly before the mid-century (e.g., see Kerr, 2009). The removal of ice would certainly alter deposition processes for particulate Hg(II) but would also provide a stronger evasion of Hg(o) (e.g., see Andersson et al., 2008). Stronger Hg(o) evasion, together with greater opportunity for photo reduction, would favor a decrease in the net deposition of Hg, with effects on the Hg inventories in the upper ocean similar to those resulting from emissions reductions of up to 20%.

7.5. How feasible and costly will be future global mercury emission reductions?

Measures available for reducing Hg emissions differ with regard to emission control efficiency and cost. Costs and benefits associated with Hg emission reductions from major anthropogenic sources were assessed by Pacyna et al. (2010b). They concluded that measures that include the application of technology, such as technology to remove Hg from flue gases in electric power plants, waste incinerators, and smelters, are expensive compared to non-technological measures such as prevention activity and promotion of Hg-containing waste separation. However, some technologies can be relatively inexpensive when used as an incremental approach with other pollutant-reduction measures. Economic benefits from decreasing Hg emissions were estimated by Sundseth et al. (2010). They suggested that the annual global cost would be approximately USD 3.7 billion (2005) based merely on loss of IQ (Intelligent Quotient) from exposure to methylmercury if the present projector for 2020 is maintained. Table 7.8 summarizes the qualitative costs and benefits assessment of the major by-product emission categories as presented by Pacyna et al. (2010b)

At present, it is uncommon to invest in technologies to reduce only Hg from the emissions stream. Instead, a multi-pollutant approach is commonly used, which is much more cost effective. For example, approaches and technologies for controlling conventional air pollutants, including particulate

Table 7.8. A qualitative assessment of the costs and benefits from different mercury by-product reduction options. Source: Pacyna et al. (2010b).

Reduction option	Costs	Benefits
1 Reduction from coal usage	Medium → Large	Large
2 Reduction from industrial processes	Medium → Large	Medium → Large
3 Reduction from waste	Small → Large	Large
4 Reduction from chlor-alkali industry	Small → Large	Medium → Large

matter, sulfur dioxide and nitrogen oxides, typically result in some reduction of Hg emissions as a co-benefit. In most cases, Hg controls are contingent upon controls for conventional pollutants, although the degree of the Hg capture by various technologies varies widely. In this context, the incremental cost of adding a Hg reduction effort to a certain strategy is much smaller.

Efficient, non-technological measures and pre-treatment methods are also available for the reduction of Hg releases from various uses of products containing Hg. These measures include bans on use and substitution of products containing Hg and cleaning of raw materials before their use (e.g., coal cleaning). These measures also include energy conservation options, such as energy taxes, consumer information, energy management, and improvement of efficiency of energy production through a co-generation of electricity and heat in coal-fired power plants. Other potential measures affecting Hg emissions also comprise prevention options aimed at reducing Hg in wastes, material separation, labeling of Hg-containing products, and input taxes on the use of Hg in products.

The message from the review of abatement installations for reduction of Hg emissions from various anthropogenic sources from UNEP's second Ad Hoc Open-ended Working Group on Mercury, is that there are a number of technological and non-technological solutions available that could be employed at present in order to reduce Hg emissions by 2020. Of course, it is expected that even more technological measures will be available in the near future, particularly in the field of application of renewable sources of energy production and the improvement of Hg removal using the 'add on' measures in addition to electrostatic precipitators (ESPs) / fabric filters (FFs) combined with various types of flue gas desulfurization (FGDs). There is also a great potential for improvement of non-technological measures such as decrease in the use of Hg in the future and development of incentives for application of measures aiming at reduction of Hg emissions to the environment.

7.5.1. Mercury emission reductions from coal combustion

In coal-burning facilities, any viable means to improve the efficiency of the plant should be considered for controlling Hg emissions. Improvement of plant efficiency also provides for reduction of greenhouse gas emissions in addition to reduction of Hg emissions. Some of the most commonly applicable measures at a coal-burning facility include: new burners, improved air preheater, improved economizer, improved combustion measures, minimization of short cycling, minimization of gas-side heat transfer surface deposits, and minimization of air infiltration. In addition, operation and

maintenance practices have a significant impact on plant performance, including its efficiency, reliability, and operating cost. Depending on the coal used, a certain decrease in Hg emissions may be obtained by the deployment of coal treatment technologies prior to combustion. Coal treatment technologies considered in the context of plant efficiency and Hg removal, include conventional coal washing, coal beneficiation for Hg content, coal blending, and coal additives. Fuel substitution schemes are also capable of delivering decreased Hg emissions (e.g., substitution of coal with natural gas or renewable energy sources).

Next, secondary measures should be applied, that is, a set of approaches designed to maximize the so-called co-benefit removal, or the amount of Hg removal that is realized as the effect of operation of air pollution control equipment originally designed to limit emissions of criteria pollutants (particulate matter, sulfur dioxide and nitrogen oxides) and already in place at the power plant (Table 7.9). Depending on the available air pollution control equipment, these approaches could include modernization of ESPs, modification of wet desulfurization scrubber chemistry, alteration of selective catalytic reduction (SCR) operation, or a combination of these.

For plants where the amount of Hg capture desired is beyond what can be achieved through co-benefit removal, deployment of dedicated Hg control technologies may be required. To date, use of sorbent injection has shown the most promise as a near-term Hg control technology. In the basic scenario envisioned for sorbent injection, powdered activated carbon is injected between the air heater and the particulate control device.

The incremental cost of Hg reduction (i.e., the cost, in USD per kg Hg removed, to achieve a specific reduction) is influenced largely by the level of baseline Hg capture exhibited by the existing air pollution control device (APCD) configuration and coal Hg content. For example, the incremental cost of Hg control will increase when: (i) baseline Hg capture by existing APCD is high, or (ii) the coal Hg content is low, because a smaller quantity of Hg is removed from the flue gas for a given level of control. The incremental cost of Hg emission reduction varies substantially depending on factors such as type of coal used, type of combustion unit, type of APCD already in place to control other pollutants, facility configuration, and percentage reductions expected from the existing APCD. For example, wet scrubbers installed primarily for Hg have been estimated to cost between USD 76 000 and 174 000 per pound of Hg removed (or USD 168 000 to 384 000 per kg of Hg removed). This result is very close to the cost of USD 234 000 per kg of Hg removed, estimated and used in a study of the effectiveness of the UNECE Heavy Metals Protocol and cost of additional measures.

Early estimates of Hg control costs indicated that it would cost between USD 67 700 and 70 000 per pound (or USD

Table 7.9. Average mercury capture by existing post-combustion control configurations installed on coal-fired units. As presented in Pacyna et al. (2010b).

Post-combustion control strategy	Post-combustion emission control device configuration	Average mercury capture by control configuration, %		
		Coal burned in PC-fired boiler unit		
		Bituminous coal	Subbituminous coal	Lignite
PM control only	ESPC	36	9	1
	ESPh	14	7	not tested
	FF	90	72	not tested
	PS	not tested	9	not tested
PM control and spray dryer absorber	SDA + ESP	not tested	43	not tested
	SDA + FF	98	25	2
	SDA + FF + SCR	98	not tested	not tested
PM control and wet FGD System ^a	PS + FGD	12	10	not tested
	ESPC + FGD	81	29	48
	ESPh + FGD	46	20	not tested
	FF + FGD	98	not tested	not tested

^a Estimated capture across both control devices. ESPC = cold-side electrostatic precipitator; ESPh = hot-side electrostatic precipitator; FF = fabric filter; PS = particle scrubber; SDA = spray dryer absorber system.

149 300 to 154 000 per kg) to achieve a 90% control level using sorbent injection. However, following the Research, Development and Demonstration (RD&D) activities sponsored by the US Department of Energy (DOE), the costs of sorbent injection for Hg removal have shown significant advances along with the potential for reductions in overall installation and operational costs. A DOE economic analysis released in 2007 indicated that the cost of Hg control could be drastically lowered compared to original estimates due to a reduction in the injection rate of a sorbent. The analysis indicated that a levelized incremental cost of 90% Hg emission control by means of powdered activated carbon injection ranged from about USD 30 000 to less than USD 10 000 per pound of Hg removed for DOE field testing sites¹. These DOE test sites used a chemically-treated (brominated) activated carbon. While the capital cost of a Hg control system (i.e., activated carbon injection; ACI) is relatively low, the major expenditure comes from the cost of carbon itself. Generally, brominated carbon affords much lower injection rates (mass sorbent / flue gas flow) than the untreated carbon to accomplish the same level of Hg removal. Thus, despite the fact that chemically treated carbons are more expensive than untreated ones, the use of chemically treated carbons allows a significant reduction in the cost of Hg removal.

7.5.2. Mercury emission reductions from industrial processes

Abatement costs for reduction of heavy metals, including Hg, within various industries were assessed for the heavy metal emission reduction Protocol of the UNECE Convention on Long-range Transboundary Air Pollution. The results of this assessment are similar to the data presented in Table 7.10.

Industrial processes contribute about 25% to the total emissions of anthropogenic Hg to the atmosphere (UNEP,

2008). Emissions from the non-ferrous and ferrous metal industries are estimated to contribute about 10% each to the total emissions. With regard to Hg emissions from non-ferrous metal production, amounts depend mainly on: (i) the Hg content of non-ferrous metal ores used mostly in primary processes or scrap used in secondary non-ferrous production, (ii) the type of industrial technology employed in the production of non-ferrous metals, and (iii) the type and efficiency of the emission control installations.

The content of Hg in ores varies widely from one ore field to another (e.g., Pacyna, 1986) as does the Hg content of scrap. Depending on the country, Hg emissions from primary production using ores in non-ferrous smelters are between one and two orders of magnitude higher than the Hg emissions from secondary smelters with scrap metal as the main raw material. Pyro-metallurgical processes in the primary production of non-ferrous metals, employing high temperature roasting and thermal smelting, emit Hg and other raw material impurities, mostly to the atmosphere. Non-ferrous metal production with electrolytic extraction is responsible more for risks of water contamination.

The primary sources of Hg emissions from cement manufacturing contribute about 10% to the total anthropogenic emissions of this element. Mercury emissions are mostly generated during the processing of raw materials in the kiln. Kiln operations consist of pyro-processing (thermal treatment) of raw materials, which are transformed into clinkers. Raw material processing differs for the wet- and dry-kiln processes. Regardless of kiln type, Hg is introduced into the kiln with raw material (limestone) and with fuels (e.g., coal), which are used to provide heat for calcination and sintering of raw materials. Other fuels, such as shredded municipal garbage, chipped rubber, petroleum coke, and waste solvents, are also frequently used and may contribute to Hg emission from cement production.

In addition, fly ash from coal combustion may be added to clinker for concrete production. This added fly ash may contain Hg as a result of the condensation of gaseous Hg on fine fly ash particles in the flue gas before the collection of fly

¹ Potential loss of revenue for plants that sell fly ash for beneficial reuse (e.g., in concrete manufacture) is not taken into account. An increase of 172–300 % on the Hg removal cost has been indicated if relevant (NESCAUM, 2010).

Table 7.10. Maximum and minimum annual costs for technological reduction of mercury in various source sectors as calculated within the EU ESPREME project (ESPREME, 2007). Capital costs are calculated with the assumption of a 15-year technology lifetime and a 4% discount factor, assumptions on inflation included.

Sector	Specific activity indicator (SAI)	Minimum percentage Hg reduction	Maximum percentage Hg reduction	Minimum annual costs, USD 2008/SAI	Maximum annual costs, USD 2008/SAI
Coal combustion	MWh	24	98	1.4	5.7
Sintering	metric ton sinter	5	99	0.2	3.2
Primary lead	metric ton primary lead	5	90	0.1	3.8
Primary zinc	metric ton primary zinc	5	10	0.2	5.6
Primary copper	metric ton primary copper	5	10	15.6	29.5
Secondary lead	metric ton secondary lead	5	10	0.2	7.9
Secondary zinc	metric ton secondary zinc	5	10	0.2	1.5
Secondary copper	metric ton secondary copper	5	10	26.8	50.6
Cement production	metric ton cement	5	98	0.4	1.8
Coke production	metric ton coke	5	98	0.02	3.0
Pig iron production	metric ton cast iron	5	72	1.0	6.0
Iron and steel foundry	metric ton cast iron	5	98	93.6	148.8
Electric arc furnace steel	metric ton steel	98	98	1.7	1.7
Basic oxygen furnace steel	metric ton steel	5	70	4.2	8.8
Waste incineration	metric ton waste	20	99	0.2	12.7
Chlorine production ^a	metric ton chlorine	15	100	0.04	37.0

^a Mercury cell plants.

ash in particulate control devices, such as ESPs or FFs. The US Environmental Protection Agency reported that Hg is retained by fly ash from the use of sorbents for enhanced Hg capture, and is thus unlikely to be leached into the environment (US EPA, 2006). The same was also found to be the case for wet FGD scrubbers (US EPA, 2008).

Large non-ferrous smelters use high efficiency air pollution control devices to control particulate matter and sulfur dioxide emissions from roasters, smelting furnaces, and convertors. Electrostatic precipitators are the most commonly used devices for the control of particulates. Mercury is emitted mostly in a gaseous elemental form from large non-ferrous smelters, and therefore, the ESPs are not very effective in its removal. The elemental Hg does not end up in sulfuric acid plants and is instead emitted to the atmosphere from the smelter stacks. The amount of these emissions depends on the Hg content of the ore. This varies widely from one ore field to another. Because Hg emissions are mostly in the elemental form, ACI or wet scrubbers may be needed to control them. Other options to control Hg emissions from industrial sources include those discussed for the coal combustion sector.

Mercury can be emitted to the atmosphere during the production of metallurgical coke, which is used in the iron and steel industry. Electrostatic precipitators or FFs and, less frequently wet scrubbers, are used in the coke production plants to control emissions, particularly those generated during quenching. Quenching is performed to cool down coke and to prevent complete combustion of coke upon exposure to air. Although no data are available for the performance of ESPs and FFs in coke production plants, it is expected that Hg removal is limited. Thus, ACI would need to be deployed to control Hg emissions from metallurgical coke production facilities.

A major review of information on the costs of abatement for coal combustion and other economic sectors was carried out within the EU ESPREME (<http://espreme.iwr.uni-stuttgart.de>) and DROPS (<http://drops.nilu.no>) projects.

The annualized investment and operational costs for installations that are used to remove Hg, including ESPs, FFs, FGD, and 'add on' measures just for Hg removal are presented in Table 7.10. The accuracy of cost estimates in Table 7.10 is within $\pm 50\%$ as calculated within the EU ESPREME project. These costs are given in relation to the production of 1 t of specific production and are indicated in Table 7.10 as a specific activity indicator. The information on efficiency of Hg removal using these installations is also included in Table 7.10.

Industrial sources of Hg emissions often include small industrial boilers. Because of the economy of scale, different control strategies may be needed for these small industrial boilers than for large industrial sources or for coal-burning utility power plants. Major assessment of costs and environmental effectiveness of options for reducing Hg emissions to air from small-scale combustion installations (<50 MWh) was prepared for the European Commission by Pye et al. (2005). Pye and co-workers concluded that preventive options were one of the most cost-effective options (e.g., options prior to combustion to minimize emissions), such as coal washing and fuel switching. Such options require the use of a better quality, cleaner fuel within the same fuel type, or switching to a different type of fuel with a lower Hg content and resultant emissions.

Another preventive option is reduction in energy consumption through energy efficiency, as discussed for the coal combustion sector. Only limited technical abatement options (such as removal of Hg from flue gases after combustion) were identified for small-scale combustion installations.

An assessment of abatement costs for reduction of heavy metals, including Hg, within various industries was undertaken for the heavy metal emission reduction Protocol of the UNECE Convention on Long-range Transboundary Air Pollution (Visschedijk et al., 2006). The results of this assessment are similar to the data presented in Table 7.10.

7.6. Conclusions and recommendations

Conclusions (in numbered bullets) are organized under section headings, followed by knowledge gaps / recommendations (in italics) when appropriate.

How are anthropogenic mercury emissions likely to change in the future?

1. An increase equivalent to about one quarter of the 2005 global anthropogenic Hg emissions, or about 500 t per year, is expected by 2020 if there are no major changes in economic trends or in the efficiency of emission controls (i.e. the SQ or 'business as usual' option).
2. Alternately, the widespread implementation of available control technologies (the 'EXEC' or the more stringent 'MFTR' options) could reduce global Hg emissions by up to 60% by 2020 compared to current practices.

More accurate assessment of future scenarios is needed. In particular, there is a need to take into account different energy mixes and changes in terms of the increased use of renewable energy. More complete emission inventories are also needed with regard to intentional use- and by-product emission sources, especially for intentional use of Hg in products.

Emissions scenarios for 2050 and 2100 should be estimated to give an idea of long-term future trends under different scenarios, and more accurate information on economic and social variables worldwide should be introduced into the emissions scenarios.

How will future changes in global emissions and climate affect mercury levels in the Arctic atmosphere?

3. The average increase in atmospheric gaseous Hg (GEM) concentrations in the Arctic and sub-Arctic between 2005 and 2020 under the 'business as usual' emissions scenario is relatively small (~3%), but increases in deposition (up to ~5%) will be slightly higher because of the predicted greater proportion of oxidized anthropogenic Hg in Arctic air which has a faster deposition rate than GEM.
4. Similarly, the decreases in atmospheric Hg deposition in the Arctic by 2020 achieved under the EXEC and MFTR control scenarios will be greater than those in GEM concentrations, because of proportionately larger reductions in emissions of oxidized Hg species.

Model parameterization (e.g., emissions data, meteorological conditions, and inclusion of natural emissions and re-emissions in the models) should be improved.

What will be the recovery time for mercury in the Arctic atmosphere and ocean under future scenarios of emissions reductions?

5. It may take 15 years for the atmospheric deposition of Hg in the Arctic to be reduced by 20% relative to levels in 2005.
6. For a 5% reduction in atmospheric deposition between 2005 and 2020, Arctic Ocean surface water inventories may be reduced by 2.4% on average in the western Arctic Ocean and 2.1% in the eastern Arctic Ocean. A 20% emissions reduction

between 2005 and 2020 is predicted to produce reductions of 9.5% and 8.3% in average seawater Hg concentrations, respectively.

7. Owing to the large mass of Hg involved, and the slow turn-over times of deep-ocean waters, total clearance of anthropogenic Hg from the whole Arctic Ocean is expected to take decades to centuries to achieve following significant emissions reductions. More rapid responses are likely to occur in surface waters down to 200 m depth.

Extensive use of models is needed for relating changes in Hg emissions to changes in concentration in the Arctic. Research should be adapted to improve the dose-response functions needed for assessing biological recovery; more accurate information on speciation will give more accurate information on dose-response relationships.

How feasible and costly will be future global mercury emission reductions?

8. Measures for reducing Hg emissions are available, but some removal technologies are rather expensive. A multi-pollutant approach is commonly used for removing Hg from the emissions stream and is more cost-effective. Non-technological methods and pre-treatment of raw materials can be used in combination with technical measures.

Further assessment of the benefits in the Arctic resulting from global Hg emissions reductions is needed to improve the basis for cost-bearing decisions that are taken to achieve Hg reductions. Improved information should also be obtained on costs and benefits of multi-pollutant reduction measures.

General recommendations

- Invite research funding agencies to prioritize improvements to Hg emissions scenarios and projections.
- Undertake research on Hg emissions, concentrations of Hg, and impacts of Hg in the Arctic environment.
- Investigate the socio-economic consequences in the Arctic of global Hg emissions. Address changes in Arctic Hg contamination within the context of climate change.